Antarctic ice sheet thickness estimation using the H/V spectral ratio method with single-station seismic ambient noise

Peng Yan[1], **Zhiwei Li**[2], **Fei Li**[1,3*], **Yuande Yang**[1], **Weifeng Hao**[1], **Feng Bao**[2]

[1]Chinese Antarctic Center of Surveying and Mapping, Wuhan University, Wuhan 430079, China
[2]State Key Laboratory of Geodesy and Earth's Dynamics, Institute of Geodesy and Geophysics, Chinese Academy of Sciences, Wuhan 430077, China
[3]State Key Laboratory of Information Engineering in Surveying, Mapping and Remote Sensing, Wuhan University, Wuhan 430079, China

Correspondence to: Fei Li (fli@whu.edu.cn)

Abstract. The horizontal-to-vertical spectral ratio (H/V) method implemented at single stations using seismic ambient noise waveforms is a fast, noninvasive, efficient method to investigate the subsurface velocity structures of the shallow crust. In this study, we report on a successful application of the H/V method to estimate the Antarctic ice sheet thickness for the first time. Using three-component, five-day long, seismic ambient noise records gathered from more than 60 temporary seismic stations located on the Antarctic ice sheet, the ice thickness at each station was reliably measured. Preliminary analysis revealed that 60 out of 65 seismic stations on the ice sheet obtained clear peak frequencies (f_0) related to the ice sheet thickness in the H/V spectrum. Thus, assuming that the isotropic ice layer lies atop a high velocity half-space bedrock, the ice sheet thickness can be calculated by a simple approximation formula. About half of the calculated ice sheet thickness were consistent with the Bedmap2 ice thickness values. To further improve the reliability of ice thickness measurements, two-type models were built to fit the observed H/V spectrum through non-linear inversion. The two-type models represent the isotropic structures of single and two-layer ice sheet, and the latter depicts the non-uniform, layered characteristics of the ice sheet widely distributed in Antarctica. The inversion results suggest that the ice thicknesses derived from the two-layer ice models were highly consistent with the Bedmap2 ice thickness database, and their ice thickness differences were within 300 m at almost all stations. Our results support previous finding that the Antarctic ice sheet is stratified. Extensive data processing indicates that the time length of seismic ambient noise records can be shortened to 1—2 hours for reliable ice sheet thickness estimation using the H/V method. This study extends the application fields of the H/V method and provides a complementary and independent way to measure ice sheet thickness in Antarctica.

1 Introduction

The Antarctic ice sheet is the largest on the Earth, covering over 98 % of Antarctic continent. As a fundamental parameter of the Antarctic ice sheet, ice sheet thickness is significant for dynamic ice sheet modeling of mass

33 balance and global climate change (Budd et al., 1991; Gogineni et al., 2001; Bamber et al., 2001; Hanna et al.,
34 2013). Moreover, seismic waves become more complex when traveling through an ice sheet with thickness
35 ranging in hundreds to thousands of meters thick. Thus, accurate ice sheet thickness is a critical metric for
36 recognizing and denoising seismic multiples trapped inside the ice sheet when imaging crustal and mantle
37 structures below the ice sheet (Lawrence et al., 2006; Hansen et al., 2009, 2010). Therefore, better ice sheet
38 thickness and structures can also improve the study of the geological structure underneath the ice sheet in
39 Antarctica.

40   Given the importance of Antarctic ice sheet structures, many geophysical methods, such as gravity modeling,
41 radio echo sounding (RES), and active seismic approaches including reflection, refraction, and deep seismic
42 sounding, have been used in local or regional scale ice sheet thickness investigations since the 1950s (Bentley
43 and Ostenso, 1961; Bentley, 1964; Evans and Robin, 1966; Evans and Smith, 1969; Robin, 1972; Drewry et al.,
44 1982; Cui et al., 2016). By studying gravitational anomalies in the ice sheet, gravimetric measurements provide
45 an indirect way to infer the average ice thickness over a region. While active seismic and RES methods can
46 determine the ice thickness at a much smaller area by converting the echo time of seismic and electromagnetic
47 waves into an estimation of ice thickness. Among these methods, the active seismic and RES methods are the
48 most widely used techniques for ice thickness measurements due to their relatively high accuracy and better
49 spatial resolution. After compiling and gridding the data derived from these methods, the Bedmap1 at a
50 resolution of 5 km and Bedmap2 at a resolution of 1 km ice sheet thickness databases covering south of 60° S
51 were constructed (Lythe et al., 2001; Fretwell et al., 2013). However, traditional methods for estimating ice
52 thickness still have limitations. For example, the accuracy of the gravity method is relatively low because of its
53 intrinsically low sensitivity of a gravimeter to the gravitational anomalies related to the ice sheet-bedrock
54 interface and the approximated terrain correction assumptions necessary for data processing (Drewry, 1975). In
55 the case of the active seismic and RES methods, despite their high accuracy they require considerable economic
56 and logistical support, to collect the data. The RES method has a further limitation as the echo free zone (EFZ) in
57 areas of high temperature ice, possibly related to signal scattering or signal disappearance, making data
58 collection impossible in these areas (Drews et al., 2009). To enrich the ice thickness database in Antarctica and
59 make a complementary for the existing methods, more geophysical methods have to be explored for determining
60 ice sheet thickness reliably, accurately, and efficiently at low cost.

61   Passive seismic methods, such as the teleseismic P-wave receiver function (PRF), generally used to determine
62 crustal and mantle discontinuities is also sensitive to the ice-bedrock interface and the seismic properties of ice
63 sheets. Hansen (2010) successfully modeled ice sheet thickness beneath several stations in East Antarctica using
64 PRF. Wittlinger (2012, 2015) investigated the anisotropy of the polar ice sheet by modeling the P-to-S wave
65 conversion with the negative PRF amplitude. Yan (2017) confirmed that the ice thickness results derived from
66 PRF are consistent with the Bedmap2 ice thickness database. However, large numbers of teleseismic events are

67   needed to perform PRF; it usually takes at least a one-year period of data collection, thus greatly limiting the

68   application of the PRF method in harsh environments such as those found in Antarctica.

69   In order to improve the reliability, accuracy, and efficiency of ice thickness investigation, we selected the

70   horizontal-to-vertical spectral ratio (H/V) method to determine ice thickness. As a noninvasive and passive

71   seismic method, the H/V technique has been extensively used in seismic exploration as a tool to detect sediment

72   thickness, which suggests its powerful effectiveness in subsurface structure investigations (Konno and Ohmachi,

73   1998; Ibs-von Seht and Wohlenberg, 1999; Bonnefoy-Claudet et al., 2006; Bao et al., 2017). Considering that

74   the sediments and ice sheet layer are both low shear-wave velocity (Vs) layers atop the high velocity bedrock,

75   the H/V method should be suitable for determining ice sheet thickness.

76   Jean-Jacques (2010) applied the H/V method to four stations in the Dome C region of Antarctica for inferring

77   the uppermost snow layer thickness and its corresponding ice properties a few meters depth. Picotti (2017)

78   recently adopted the H/V method to detect glacial ice thickness ranging from a few tens of meters to ~800 m in

79   Italy, Switzerland, and West Antarctica. The H/V method has been validated for its reliability to measure glacial

80   thickness comparing with the radio-echo sounding, geoelectric, and active seismic methods implemented at or

81   near the same study sites. The great advantage of the H/V method over other approaches is that there is no need

82   to record earthquakes or active sources, since it utilizes seismic ambient noise. Moreover, the H/V method

83   requires only a few tens of minutes of seismic ambient noise recordings at single portable three-component

84   seismometers. This greatly enhances efficiency and reduces cost and logistical support requirements.

85   Since the shear-wave velocity of an ice sheet is ~1900 m s^{-1}, and generally much higher than a snow layer

86   (~700 m s^{-1}), therefore the velocity contrast of the ice sheet-bedrock half-space is not as high as that of the

87   snow-ice sheet layer. Moreover, the H/V spectrum may be more complicated than that of a glacier or snow layer

88   given the complex subglacial environment since there might be subglacial lakes and sedimentary layers. In

89   addition, the internal ice structure might affect the H/V spectrum given the variations in seismic velocities

90   induced by changes in density, and temperature, as well as the ice crystal size and orientation of an ice sheet.

91   Whether the H/V method can be used to estimate the ice sheet thickness or not remains an open question.

92   Although the H/V method has been successfully applied to study snow and shallow glacial thickness

93   (Jean-Jacques et al., 2010; Picotti et al., 2017), to our knowledge, the H/V method has not been performed to

94   estimate Antarctic ice sheet thickness yet. In this study, we present estimated ice thickness results from 65

95   stations with a typical coverage deployed on the Antarctic ice sheet to verify the feasibility of using the H/V

96   method as an effective complementary way to existing methods for measuring ice thickness.

2 Data and methods

2.1 Data

Over the past two decades, several temporary seismic arrays have been deployed in Antarctica, including the Transantarctic Mountains Seismic Experiment (TAMSEIS, 2000—2003) (Lawrence et al.,2006), the Gamburtsev Antarctic Mountains Seismic Experiment (GAMSEIS, 2007—2012) (Hansen et al.,2010), and the Polar Earth Observing Network/Antarctic Network (POLENET/ANET,2007—2016) (Chaput et al.,2014). Despite their relatively sparse distribution, these three arrays together effectively cover East, and West Antarctica as well as the Transantarctic Mountain region (Fig. 1). In these three arrays, all stations are equipped with the Güralp CMG-3T or Nanometrics T-240 broadband sensors with a sampling rate of 25 Hz or 40 Hz. Most stations are buried 1—2 meters below the surface snow to guarantee data quality (Anthony et al., 2015). Equipped with solar panels and rechargeable batteries, the GAMSEIS and POLENET/ANET stations work continuously year round except the TAMSEIS, and provide abundant seismic ambient noise waveforms for the H/V processing. To investigate the effectiveness of the H/V method for ice thickness measurements and the proper time length for H/V processing, we selected seismic ambient noise records lasting about five days, which is much longer than that used in usual H/V data processing (only a few minutes' records for sedimentary investigations with tens to hundreds of meters thick). In total, 65 stations deployed on the Antarctic ice sheet were used in this study.

2.2 Methods

The single-station H/V method, extensively used in sediment structure detection, acquires reliable sediment thickness and shear-wave velocities (Nogoshi and Igarashi, 1971;Nakamura, 1989). In this method, seismic ambient noise data are collected by a three component seismometer and the ratio between the horizontal (H) and vertical (V) Fourier spectra are calculated. The principle of the technique can be understood by assuming a low velocity sedimentary layer overlying a high velocity bedrock half-space. Due to the sharp impedance contrast at the interface between the two layers, the shear-wave energy within the sedimentary layer produces a prominent peak that can be observed in the H/V spectrum.

Extensive field experiments and numerical simulations have been carried out to verify the reliability of the H/V spectrum as derived from the H/V method. Although the amplitude value of the H/V spectrum peak frequency is not that robust since the contributing factors are complicated, the H/V spectrum peak frequency is commonly accepted as a proxy of the resonance frequency of a particular layer (Field and Jacob, 1993; Lachetl and Bard., 1994; Javier and Chávez-García, 1994; Delgado et al., 2000; Fäh et al., 2001; Lunedei and Malischewsky, 2015; Picotti et al., 2017). To calculate the H/V spectrum, a specialized GEOPSY program was developed by the European SESAME team, and widely used to investigate the sediment structures (Bard and

129   SESAME team, 2005). Then an approximation equation or H/V spectrum inversion approach can be used to

130   derive the sedimentary layer thickness with the H/V spectrum.

131   Under the assumption of one-dimensional velocity subsurface conditions, in cases of homogenous and

132   isotropic sedimentary layers over a homogenous half-space, the observed peak frequency equals the

133   fundamental resonant frequency of the sedimentary layer. Thus, the resonance frequency of the low velocity

134   layer is closely related to its thickness h through the following relationship (Ibs-von Seht and Wohlenberg, 1999;

135   Parolai et al., 2002; Picotti et al., 2017; Civico et al., 2017):

136
$$h = \frac{Vs}{4 f_0} \tag{1}$$

137   Where Vs is the average shear-wave velocity of the sedimentary layer, and f_0 is the observed peak frequency.

138   Provided that a correct estimate of the average shear-wave velocity of the sedimentary layer is available, its

139   thickness can be roughly estimated.

140   Complicated sedimentary internal structures, including anisotropy and low velocity layers beneath stations,

141   will affect the H/V spectrum and consequently violate the assumptions of Eq. (1). Therefore, when inferring

142   complex subsurface structures, an inversion of the full H/V spectrum can be used to explain more accurately the

143   observed H/V spectrum. Based on different assumptions for the interpretation of ambient noise wavefield

144   composition, several inversion approaches have been proposed and successfully applied to study sedimentary

145   structures (Fäh et al., 2003; Arai and Tokimatsu, 2004; Herak, 2008; Lunedei and Albarello, 2009;

146   Sánchez-Sesma et al., 2011).

147   The H/V method has been successfully applied in studies of sedimentary structures, such as studies of

148   thickness and shear- wave velocities (Ibs-von Seht and Wohlenberg, 1999; Langston and Horton, 2014; Civico

149   et al., 2017; Bao et al., 2017). However, applications in ice environments are rare. Jean-Jacques (2010) studied

150   the snow layer thickness and the ice properties beneath four stations in Dome C region of Antarctica using the

151   H/V method. Picotti (2017) measured ice thickness ranging from tens of meters to 800 m of six glaciers in Italy,

152   Switzerland and West Antarctica. However, the impedance contrast between the ice sheet layer and the

153   overlying bedrock is not as high as that of sedimentary-bedrock and snow-ice layers. Moreover, the complex

154   subglacial environment and internal ice structure create other technical obstacles. Thus, there have been no

155   investigations of ice sheet thickness incorporating the H/V method for measurements or estimations.

156   In this study, the H/V spectra of 65 stations deployed on ice were processed by using the GEOPSY software,

157   which has been used for sedimentary structure investigations in many regions. Under the general assumption

158   that the seismic properties are stable throughout the whole ice column, we calculated the ice thickness using Eq.

159   (1) as in most seismological applications to approximate the ice sheet as a homogeneous layer. Meanwhile, a

160   non-linear H/V spectrum inversion method developed by García-Jerez (2016) was adopted to constrain the

161   observed H/V spectrum to infer the ice structure, comprised of shear-wave velocity and thickness.

162   During H/V spectrum acquisition using the Geopsy software, we remove the transient signals (earthquakes)

163   from noise records with the STA/LTA technique and divide the records into 600 s length windows with an

164   overlap of 5 %. Time series were tapered with a 5 % cosine function, and the FFT was calculated for each

165   component. The spectra were smoothed with a Hanning window in a bandwidth of 0.1—2 Hz on a logarithmic

166   frequency scale. The spectra of the two horizontal components (NS and EW) were merged to one horizontal

167   component spectrum by calculating their geometric mean. The spectral ratios and corresponding standard

168   deviation estimates between the horizontal component and the vertical component were calculated.

169   Having acquired the resonance frequency of the ice sheet, we adopted Eq. (1) with a uniform average

170   shear-wave velocity—1900 m s^{-1} of the ice layer to calculate the ice thickness. This velocity used here is

171   reasonable given that it is in the general range of ice Vs determined by seismic experiments (Kim et al., 2010).

172   Moreover, this velocity has also been widely used in previous studies (Hansen et al., 2010; Wittlinger and Farra,

173   2012; Ramirez et al., 2016). Keeping the velocities set, the ice thickness at each station was calculated using Eq.

174   (1).

175   In the H/V spectrum inversion procedures, Bedmap2 ice thicknesses were used as references to build the

176   initial models, as along with the related seismic elastic parameters (Fig. 2, Wittlinger and Farra, 2012; Ramirez

177   et al., 2016). We adopted two different models assuming the ice sheet is homogenous and inner ice stratified;

178   respectively, as shown in Fig. 2 to perform H/V spectrum inversion. Model A is a simple homogeneous and

179   isotropic ice structure with an ice layer overlying the half-space. In this model, the ice thickness varies from 0.7

180   to 1.3 times the Bedmap2 ice thickness for each station. Model B is constructed following Wittlinger (2012,

181   2015) as a two-layer ice structure in which a low shear-wave velocity lies in the lower ice layer. In this model,

182   the thickness of the upper ice layer and the lower ice layer were set to occupy 60—75 and 25—40 percent of the

183   Bedmap2 thickness, respectively. Using the non-linear Monte Carlo method (García-Jerez et al., 2016), we

184   retrieved the optimum solutions for model A and B. These two solutions were best fitted to the observed H/V

185   spectum.

186   It usually takes a few minutes to about half an hour to collect seismic ambient noise waveforms in the

187   investigations of sedimentary layers with thickness ranging from several tens to hundreds of meters. However,

188   there is no experiences for the time length of recording seismic ambient noise in the Antarctic ice sheet with

189   several kilometers thick. It is necessary to apply the H/V method with a much shorter recording time for seismic

190   ambient noise, considering the harsh environment and logistical support difficulties in Antarctica. Therefore, we

191   investigated the feasibility and reliability of H/V method by testing a range of noise record lengths; eight hour,

192   four hour, two hour, and one hour intervals were tested. The processing strategies remained the same as in H/V

193   spectrum acquisition except the window length was changed to 200 s when calculating the H/V spectrum using

194   different length noise records.

3 Results

In this study, the H/V spectra of 65 stations were obtained. Figure 3 displays the H/V spectra of nine stations selected from three arrays. These examples are representative of all the results, and the remaining spectra are presented in the supplementary Fig. S1. It is clearly shown that in almost all H/V spectra there were two or three clear peaks in the frequency band. Generally, the largest amplitude appears at the first peak located around 0.2 Hz or below, and the second and the third peaks with lower amplitudes are located at ~0.5 and ~0.8 Hz, respectively. Following the general interpretation principles for H/V spectra (Bard and SESAME team, 2005), the peak frequency denoting the largest amplitude should be the resonance frequency of the ice sheet layer, while the peaks appearing with lower amplitudes at higher frequencies may indicate the shallower impedance contrast layers. The reasonableness of considering the first peak frequency with the largest amplitude as the resonance frequency of the ice sheet layer was verified through rough estimation based on Eq. (1), i.e., for station E012, the Bedmap2 ice thickness at that location is 1050 m, so the resonance frequency according to Eq. (1) should be 0.452 (the given Vs is 1900 m s^{-1}), and as expected was observed in the H/V spectrum. However, there are exceptions such as station N148 displayed in Fig.2 whose first peak amplitude is slightly lower than that of the following peak observed at higher frequency. At this station however, the location of the first peak correlates with the resonance frequencies through rough estimation. In addition, there are some stations that have no peak frequencies correlating with the ice sheet thickness, despite the existence of peak frequency with strong amplitude in the frequency band. Station ST07 seen in Fig. 3 is such a case, whose fundamental resonance frequency as calculated by Eq. (1) should be 0.191 (its Bedmap2 ice thickness is 2490 m). Nevertheless, no clear peak around this expected frequency is observed in the H/V spectrum. We therefore can group the results into three categories:

1) 42 stations with first peaks denoting the largest amplitude in the observed spectrum related to the ice sheet resonance frequency, like the E012, E018, GM02, N148, P071, ST01, ST02 stations in Fig. 3.

2) 18 stations with first peaks with slightly lower amplitude but also related to the ice sheet resonance frequency such as station N108.

3) Five stations without peaks correlating to the resonance frequency, such as station ST07.

Figure 4 shows the H/V spectra of stations along four profiles, together with the ice sheet and bedrock elevation extracted from Bedmap2 database for each station. As shown in Fig. 4, although the neighboring stations are 80 km apart for profile AA', 100 km for profile BB' and DD', and 20 km for profile CC', the shape of the spectra are similar along each profile. Also, along each profile, the peaks associated with the ice thickness are clear and the locations of the peaks shift towards lower or higher frequencies cohering with the variation of the corresponding ice thickness. There are four stations (N060, ST04, ST06, ST07) along the four profiles without peak frequencies related to their corresponding ice thicknesses. This may be caused by the bad coupling of the seismometer with the ice surface or possibly a complicated subglacial environment, for example clear evidence indicates the existence of sedimentary layer beneath station N060.

230   Having identified resonance frequency of the ice sheet, we calculated the ice thickness using Eq. (1) with the

231   average shear-wave velocity—1900 m s⁻¹. The results are listed in Table 1. We projected the calculated ice

232   thickness and the reference Bedmap2 ice thickness for stations along the four profiles in the upper elevation

233   panels in Fig. 4. It is clear that the calculated ice thickness for some stations along the four profiles are close to

234   the reference ice thickness like the E012, P071, and ST01 stations, while there are large deviations at some

235   stations such as E018, N148, and ST02.

236   The optimum shear-wave velocity models derived from H/V spectrum inversion are presented in Fig. 5 and

237   supplementary Fig. S2. The observed H/V spectrum together with the synthetic H/V spectra using the two

238   optimum shear-wave velocity models are plotted in Fig. 6 and shown in supplementary Fig. S3. As Fig. 6 and the

239   supplementary Fig. S3 shows, the synthetic H/V spectra of the optimum inversion results for model A and model

240   B at almost all stations, both fit the observed H/V spectra in peak frequency and spectrum shape. However, the

241   inversion ice thickness from model A deviates substantially from the Bedmap2 thickness at most stations (such

242   as N108, N148, GM02 and ST02 in Fig. 5), and the difference extends 1 km for some stations (Fig. 7). By

243   contrast, the inversion thickness from model B is consistent with the Bedmap2 thickness as the differences

244   between them are mostly within 200 m. The overall inversion ice thicknesses from model B are listed in Table 1.

245   We also projected the inversion thickness for stations along the four profiles in the elevation panels seen in Fig.

246   4, which depicts a high level consistency between the inversion and the reference ice thickness at these stations.

247   The results of four different length seismic ambient noise records (1 h, 2 h, 4 h, 8 h) used to obtain H/V

248   spectrum are displayed in Fig. 8 (and in supplementary Fig. S4). These plots show that the shape of the spectra of

249   the four tested record lengths are similar to the shape determined using a record five days long. The peak

250   frequencies of the four different length records are all within the margin of error for the peak frequency as

251   determined with the record five days long. We found that the longer the ambient noise record, the more stable the

252   peak frequency is as there are slight shifts in the peak frequency when determined with 1 h and 2 h records; such

253   as those from stations E018 (Fig. 8), E020, and E024 (shown in supplementary Fig. S4). Despite variation in ice

254   thickness from 600 m to about 4 km at the study sites, the length for recording seismic ambient noise suited for

255   H/V methods can be as short as 1—2 hours, in terms of stability and efficiency.

256   **4   Discussion**

257   Bedmap2 ice thickness were used as reference to verify the ice thickness derived from Eq. (1) and H/V spectrum

258   inversion since we lacked actual ice thickness as obtained from the more direct and accurate ice-core drilling,

259   RES and active seismic methods at or near each study site. Because of various factors contributing to the

260   uncertainty in the Bedmap2 database such as data coverage, basal roughness, and ice thickness measurement and

261   gridding error, however, the Bedmap2 ice thickness is not exactly accurate with uncertainty varying from site to

262   site. We obtained the uncertainty of the Bedmap2 ice thickness at each station from the grids of ice thickness

263   uncertainty (Fretwell et al., 2013, also, the uncertainty at our study sites can be roughly seen in supplementary

264 Fig. S5). A close examination of the uncertainty of the Bedmap2 ice thickness reveals that the uncertainty at 52

265 stations ranges from 59 m to about 200 m, and the uncertainty at 57 stations is below 300 m. As the accuracy of

266 the H/V method is at the same scale with the uncertainty of the Bedmap2 ice thickness at the 57 stations, the

267 Bedmap2 ice thicknesses are adequate to verify the results derived from the H/V method. The remaining three

268 stations including ST09, ST13, and ST14 are excluded for validation as the uncertainty of the reference ice

269 thickness at these stations reaches 1000 m.

270   A comparison of the inversion ice thickness from Model B and Bedmap2 database reveals that the differences

271 in ice thickness at all the 57 stations are less than 400 m; there are 33 stations whose differences are within 200 m

272 and 47 stations within 300 m; the maximum difference was 370 m at station ST03. Given that uncertainty of the

273 Bedmap2 database can reach 300 m in some study sites (Fretwell et al., 2013), it is certain that the inversion ice

274 thicknesses are adequately constrained at over 47 stations.

275   Based on the homogenous ice sheet layer assumption, most of the ice thickness estimations derived from Eq.

276 (1) are not compatible with Bedmap2 ice thickness (Fig. 4 and Fig. 7), as the differences at 26 stations can extend

277 400 m and at 10 stations are over 600 m; the maximum difference reaches 910 m at station N036. Moreover,

278 most of the inversion ice thickness results based on the homogenous ice structure of model A also largely

279 deviated from the reference Bedmap2 thickness (Fig. 7 and supplementary Fig. S2). These large deviations

280 cannot be attributed to the uncertainty in the reference Bedmap2 ice thickness since they made minor

281 contributions to the large differences.

282   The inversion ice thickness from model B, however were highly consistent with the Bedmap2 database. A

283 close examination of the inversion thickness from model B shows that it refined the rough estimation results at

284 47 stations as calculated with Eq. (1) to varying degrees. As at stations E012 and N036, the calculated ice

285 thicknesses using Eq. (1) deviate from Bedmap2 at 90 m and 910 m, while the inversion ice thickness from

286 model B refines the gaps to 20 m and 320 m.

287   We compared our results with those found in Wittlinger (2012). Using the PRF method and a grid search

288 stacking technique, he found that the Antarctic ice is stratified, possibly due to the preferred orientation of ice

289 crystals and fine layering of soft and hard ice layers under pressure. In Fig.9, we present the ice thickness results

290 for 12 stations common to both studies. It is clear that the interface separating the upper and the lower ice sheet

291 layers determined using the H/V method and the PRF method, is consistent for almost all stations.

292   The agreement of two-layer ice sheet thickness with the Bedmap2 database, and the consistency of our results

293 to Wittlinger`s results, as well as the large deviation of ice thickness estimated using Eq. (1) and model A jointly

294 support the thesis that the two-layered ice sheet models are more reasonable than an homogeneous ice sheet layer

295 assumption. Moreover, the ice thickness of 28 stations derived from Eq. (1) were close to the reference Bedmap2

296 database. This consistency, however, does not strongly support the homogenous ice sheet layer assumption as it

297 can be attributed to the fact that the Vs values adopted in rough estimation was coincidental with the average

298 velocity of the two-layer Vs models.

299   The examples presented in this work clearly show that the H/V method with seismic ambient noise can be

300   effectively to measure ice sheet thickness. However, there are also some limitations that may affect the results.

301   Shear-wave velocity (Vs), as the key parameter for H/V spectrum inversion and rough estimation using Eq. (1),

302   will significantly affect the effectiveness and uncertainty of the H/V method. We can see from Fig. 6 that the

303   synthetic H/V spectra from the optimum Vs profiles of model A and model B for the N108, GM02 and N148

304   stations (Fig. 5), match the observed H/V spectrum. The inversion ice thickness from model A and model B at

305   these stations however, are remarkably different as the results from model B are more closely match the

306   reference Bedmap2 ice thickness than those from model A (Fig. 5). Also evident in these results is a directly

307   proportional relationship between ice thickness and the Vs as expected from Eq. (1) in rough estimation. Given a

308   ~5 percent variation in the average shear-wave speed of the ice layer, then ice sheet thickness estimation will

309   result in a similar variation such as 150 m for a station with 3 km thickness. Accurate known Vs profiles are

310   therefore prerequisites when obtaining reliable H/V spectrum inversion results, as well as for rough estimations

311   using Eq. (1).

312   It is evident that the longer the noise record, the more stable the observed peak frequency is as the sources of

313   the seismic ambient noise are more evenly distributed, spatially and temporally. This is significant for stations

314   with thin ice primarily due to the fact that thin ice sheet layers are excited by high-frequency waves such as

315   winds and other sources (Picotti et al., 2017). Thus, a longer ambient noise record can improve the stability of

316   the H/V spectrum. In our study, we found that the quality of the H/V spectrum are generally better for thick ice

317   sheet layers than for thin ice sheet such as stations BENN, E012, E018, E024, E026, and E028 with relatively

318   smaller ice thicknesses than other stations. The H/V spectra for these stations exhibited less stability when the

319   lengths of noise records decreased (Fig. 8 and supplementary Fig. S4). Also, the peak frequency obtained from a

320   one hour long record slightly deviates from the peak frequency determined with a five day record. These

321   deviations consequently could lead to uncertainties in ice thickness estimation. The efficiency and the cost of

322   noise record acquisition in Antarctica however, are equally important. In this sense, the proper record length in

323   H/V method application is 1—2 hours.

5   Conclusions

325   Given the vital role that ice sheet thickness plays in ice mass balance and global climate studies, many methods

326   have been used to estimate ice sheet thickness, obtaining abundant results. However, new methods must be

327   explored to enrich the database considering the vast area of the Antarctic ice sheet and the limitations of the

328   existing methods.

329   In this study, the H/V method is proposed as a reliable, efficient method to investigate the Antarctic ice sheet

330   thickness. The H/V method is effective for identifying the fundamental resonant frequency correlating with the

331   ice sheet thickness. In this approach, the ambient noise recording length can be as short as 1—2 hours, reducing

332   costs and increasing efficiency. Equation (1) can retrieve a fast and rough estimation of the ice thickness but

333 should be used with care since the shear-wave velocity varies at different sites. H/V spectrum inversion,

334 however, unlike estimation with Eq. (1), is robust and can obtain reliable ice thickness results with given seismic

335 properties. Moreover, the H/V spectrum inversion ice sheet thickness results are consistent with the reference

336 Bedmap2 database. Our results also support the argument that the Antarctic ice sheet has a two-layer structure.

337 The H/V method is an excellent complementary approach to the most commonly used RES and active seismic

338 methods for ice sheet thickness measurements in terms of its effectiveness. What makes this new approach most

339 attractive are the ease and economy of seismic ambient noise waveforms collection when deploying a single

340 seismometer for short time intervals. Finally, we hope that specific seismic experiments can obtain more

341 accurate shear-wave velocity profiles in the ice sheet, thus making better constraints for H/V method results.

342

343 Supplementary materials include:

344 Figure S1, S2, S3, S4, S5 in pdf format

345

346 *Competing interests.* The authors declare that they have no conflict of interest.

347

348 **Acknowledgement**

349 This work was supported by the State Key Program of National Natural Science of China under Grant 41531069,

350 the Chinese Polar Environment Comprehensive Investigation and Assessment Programs under Grant

351 CHINARE2017-02-03, and the Special Funds for Basic Scientific Research of Universities under Grant

352 2015644020201. We thank the editor, Dr. Kenny Matsuoka for his critical and helpful comments that greatly

353 improve the manuscript. Seismic data are obtained from the Incorporated Research Institutions for Seismology

354 (IRIS). Figures in this study were plotted by using Generic Mapping Tools (GMT).

355 **References:**

356 Anthony, R. E., Aster, R. C., Wiens, D., Nyblade, A., Anandakrishnan, S., Huerta, A., Winberry, J. P., Wilson,

357   T., and Rowe, C.: The seismic noise environment of Antarctica. Seismological Research Letters, 86(1),

358   89–100. 2015.

359 Arai, H., and Tokimatsu, K.: S-wave velocity profiling by inversion of microtremor H/V spectrum. Bulletin of

360   the Seismological Society of America 94.1: 53–63, 2004.

Bamber, J. L., Layberry, R. L., and Gogineni, S. P.: A new ice thickness and bed data set for the Greenland ice sheet: 1. Measurement, data reduction, and errors. Journal of Geophysical Research: Atmospheres, 106(D24): 33773–33780, 2001.

Bao, F., Li, Z. W., Zhao, J. Z., Ren, J., and Tian, B. F.: Shallow crustal structure of the Tangshan fault belt unveiled by dense seismic profile and H/V spectral ratio method. Chinese Journal of Geophysics, under review, 2017.

Bard, P. Y., and Site Effects aSsessment using AMbient Excitations Team: Report D23.12, Guidelines for the implementation of the H/V spectral ratio technique on ambient vibrations measurements, processing and interpretation, in European Commission: Research general directorate, Project No. EVG1-CT-2000-00026, SESAME, 62 pp, 2005.

Bentley, C., and Ostenso, N.: Glacial and Subglacial Topography of West Antarctica. Journal of Glaciology, 3(29), 882–911, 1961.

Bentley, C. R.: The structure of Antarctica and its ice cover, in: Research in Geophysics Vol. 2, Solid Earth and Interface Phenomena, edited by: Odishaw, H., MIT Press, Cambridge, Mass., 335–389, 1964.

Bonnefoy-Claudet, S., Cornou, C., Bard, P. Y., Cotton, F., Moczo, P., Kristek, J., and Fäh, D.: H/V ratio: a tool for site effects evaluation. Results from 1-D noise simulations. Geophysical Journal International, 167(2), 827–837, 2006.

Budd, W. F.: Antarctica and global change. Climatic Change, 18(2-3): 271–299, 1991.

Chaput, J., Aster, R. C., Huerta, A., Sun, X., Lloyd, A., Wiens, D., Nyblade, A., Anandakrishnan, S., Winberry, J. P., and Wilson, T.: The crustal thickness of West Antarctica. Journal of Geophysical Research: Solid Earth, 119(1), 378–395, 2014.

Civico, R., Sapia, V., Di Giulio, G., Villani, F., Pucci, S., Baccheschi, P., and Smedile, A.: Geometry and evolution of a fault-controlled Quaternary basin by means of TDEM and single-station ambient vibration surveys: the example of the 2009 L'Aquila earthquake area. Journal of Geophysical Research: Solid Earth, 122(3): 2236–2259, 2017.

Cui, X. B., Sun, B., Su, X. G., and Guo, J. X.: Distribution of ice thickness and subglacial topography of the "Chinese Wall" around Kunlun Station, East Antarctica. Applied Geophysics, 13(1): 209, 2016.

Drewry, D. J.: Comparison of electromagnetic and seismic-gravity ice thickness measurements in East Antarctica. Journal of Glaciology, 15: 137–150, 1975.

Drewry, D. J., Jordan, S. R., and Jankowski, E.: Measured properties of the Antarctic ice sheet: surface configuration, ice thickness, volume and bedrock characteristics. Annals of Glaciology 3.1: 83–91, 1982.

Drews, R., Eisen, O., Weikusat, I., Kipfstuhl, S., Lambrecht, A., Steinhage, D., Wilhelms, F., and Miller, H.: Layer disturbances and the radio-echo free zone in ice sheets. The Cryosphere, 3(2), 195–203, 2009.

Delgado, J., Casado, C. L., Giner, J., Estévez, A., Cuenca, A., and Molina, S.: Microtremors as a geophysical exploration tool: applications and limitations. Pure and applied geophysics 157.9: 1445–1462, 2000.

396 Evans, S., and Robin, G. Q.: Glacier depth sounding from the air. Nature, 210:883–885, 1966.

397 Evans, S., and Smith, B. M. E.: A radio echo equipment for depth sounding in polar ice sheets. Journal of
398   Physics E: Scientific Instruments 2.2: 131, 1969.

399 Fäh, D., Kind, F., and Giardini, D.: A theoretical investigation of average H/V ratios, Geophys. J. Int., 145,
400   535–549, 2001.

401 Fäh, D., Kind, F., and Giardini, D.: Inversion of local S-wave velocity structures from average H/V ratios and
402   their use for the estimation of site-effects. Journal of Seismology 7, 449–467, 2003.

403 Field, E., and Jacob, K.: The theoretical response of sedimentary layers to ambient seismic noise. Geophysical
404   research letters 20.24: 2925–2928, 1993.

405 Fretwell, P., Pritchard, H. D., Vaughan, D. G., Bamber, J. L., Barrand, N. E., Bell, R., Bianchi, C., Bingham, R.
406   G., Blankenship, D. D., Casassa, G., Catania, G., Callens, D., Conway, H., Cook, A. J., Corr, H. F. J.,
407   Damaske, D., Damm, V., Ferraccioli, F., Forsberg, R., Fujita, S., Gim, Y., Gogineni, P., Griggs, J. A.,
408   Hindmarsh, R. C. A., Holmlund, P., Holt, J. W., Jacobel, R. W., Jenkins, A., Jokat, W., Jordan, T., King, E.
409   C., Kohler, J., Krabill, W., Riger-Kusk, M., Langley, K. A., Leitchenkov, G., Leuschen, C., Luyendyk, B.
410   P., Matsuoka, K., Mouginot, J., Nitsche, F. O., Nogi, Y., Nost, O. A., Popov, S. V., Rignot, E., Rippin, D.
411   M., Rivera, A., Roberts, J., Ross, N., Siegert, M. J., Smith, A. M., Steinhage, D., Studinger, M., Sun, B.,
412   Tinto, B. K., Welch, B. C., Wilson, D., Young, D. A., Xiangbin, C., and Zirizzotti, A.: Bedmap2:
413   improved ice bed, surface and thickness datasets for Antarctica, The Cryosphere, 7, 375–393,
414   doi:10.5194/tc-7-375-2013, 2013.

415 García-Jerez, A., Piña-Flores, J., Sánchez-Sesma, F. J., Luzón, F., and Perton, M.: A computer code for forward
416   calculation and inversion of the H/V spectral ratio under the diffuse field assumption. Computers &
417   Geosciences, 97, 67–78, 2016.

418 Gogineni, S., Tammana, D., Braaten, D., Leuschen, C., Akins, T., Legarsky, J., Kanagaratnam, P., Stiles, J.,
419   Allen, C., and Jezek, K.: Coherent radar ice thickness measurements over the Greenland ice sheet. Journal
420   of Geophysical Research: Atmospheres, 106(D24), 33761–33772, 2001.

421 Hanna, E., Navarro, F. J., Pattyn, F., Domingues, C. M., Fettweis, X., Ivins, E. R., Nicholls, R. J., Ritz, C.,
422   Smith, B., Tulaczyk, S., Whitehouse, P. L., and Zwally, H. J.: Ice-sheet mass balance and climate change.
423   Nature, 498(7452), 51–59, 2013.

424 Hansen, S. E., Julia, J., Nyblade, A. A., Pyle, M. L., Wiens, D. A., and Anandakrishnan, S.: Using S wave
425   receiver functions to estimate crustal structure beneath ice sheets: An application to the Transantarctic
426   Mountains and East Antarctic craton. Geochemistry, Geophysics, Geosystems, 10(8), 2009.

427 Hansen, S. E., Nyblade, A. A., Heeszel, D. S., Wiens, D. A., Shore, P., and Kanao, M.: Crustal structure of the
428   Gamburtsev Mountains, East Antarctica, from S-wave receiver functions and Rayleigh wave phase
429   velocities. Earth and Planetary Science Letters, 300(3), 395–401, 2010.

Herak, M.: ModelHVSR-A Matlab® tool to model horizontal-to-vertical spectral ratio of ambient noise. Computers & Geosciences 34.11: 1514–1526, 2008.

Ibs-von Seht, M., and Wohlenberg, J.: Microtremor measurements used to map thickness of soft sediments. Bulletin of the Seismological Society of America 89.1: 250–259, 1999.

Javier, L., and Chávez-García, F. J.: Are microtremors useful in site response evaluation? Bulletin of the seismological society of America 84.5: 1350–1364, 1994.

Jean-Jacques, L., Maggi, A., and Souriau, A.: Seismological constraints on ice properties at Dome C, Antarctica, from horizontal to vertical spectral ratios. Antarctic Science 22.05: 572–579, 2010.

Kim, K. Y., Lee, J., Hong, M. H., Hong, J. K., Jin, Y. K., and Shon, H.: Seismic and radar investigations of Fourcade Glacier on King George Island, Antarctica. Polar Research, 29(3), 298–310, 2010.

Konno, K., and Ohmachi, T.: Ground-motion characteristics estimated from spectral ratio between horizontal and vertical components of microtremor. Bulletin of the Seismological Society of America 88.1: 228–241, 1998.

Lachetl, C., and Bard, P. Y.: Numerical and theoretical investigations on the possibilities and limitations of Nakamura's technique. Journal of Physics of the Earth 42.5: 377–397, 1994.

Lawrence, J. F., Wiens, D. A., Nyblade, A. A., Anandakrishnan, S., Shore, P. J., and Voigt, D.: Crust and upper mantle structure of the Transantarctic Mountains and surrounding regions from receiver functions, surface waves, and gravity: implications for uplift models. Geochemistry, Geophysics, Geosystems, 7(10), 2006.

Langston, C. A., and Horton, S. P.: Three-dimensional seismic-velocity model for the unconsolidated Mississippi embayment sediments from H/V ambient noise measurements. Bulletin of the Seismological Society of America, 104(5), 2349–2358, 2014.

Lunedei, E., and Albarello, D.: On the seismic noise wavefield in a weakly dissipative layered Earth. Geophysical Journal International 177, 1001–1014, 2009.

Lunedei, E., and Malischewsky, P.: A review and some new issues on the theory of the H/V technique for ambient vibrations, in: Ansal, A. (Ed.), Perspectives on European Earthquake Engineering and Seismology, Geotechnical, Geological and Earthquake Engineering, Vol. 39. Springer, Heidelberg, pp. 371–394. DOI 10.1007/978-3-319-16964-4_15, 2015.

Lythe, M. B., Vaughan, D. G., and The BEDMAP Consortium: BEDMAP: A new ice thickness and subglacial topographic model of Antarctica. Journal of Geophysical Research: Solid Earth, 106(B6): 11335–11351, 2001.

Nakamura, Y.: A method for dynamic characteristics estimation of subsurface using microtremor on the ground surface. Railway Technical Research Institute, Quarterly Reports 30.1, 1989.

Nogoshi, M., and Igarashi, T.: On the amplitude characteristics of microtremor (part 2). J. Seismol. Soc. Japan 24.1: 26–40, 1971.

464 Parolai, S., Bormann, P. and Milkereit, C.: New relationships between Vs, thickness of sediments, and
465   resonance frequency calculated by the H/V ratio of seismic noise for the Cologne area (Germany).
466   Bulletin of the seismological society of America 92.6: 2521–2527, 2002.

467 Picotti, S., Francese, R., Giorgi, M., Pettenati, F., and Carcione, J. M.: Estimation of glacier thicknesses and
468   basal properties using the horizontal-to-vertical component spectral ratio (HVSR) technique from passive
469   seismic data. Journal of Glaciology, 63(238), 229–248, 2017.

470 Ramirez, C., Nyblade, A., Hansen, S. E., Wiens, D. A., Anandakrishnan, S., Aster, R. C., Huerta, A.D., and
471   Wilson, T.: Crustal and upper-mantle structure beneath ice-covered regions in Antarctica from S-wave
472   receiver functions and implications for heat flow. Geophysical Journal International, 204(3), 1636–1648,
473   2016.

474 Robin, G. Q.: Radio-echo sounding applied to the investigation of the ice thickness and sub-ice relief of
475   Antarctica. Antarctic Geology and Geophysics: 675–682, 1972.

476 Sánchez-Sesma, F. J., Rodríguez, M., Iturrarán-Viveros, U., Luzón, F., Campillo, M., Margerin, L., Jerez,
477   García-Jerez, A., Suarez, M., Santoyo, M. A., and Rodríguez-Castellanos, A.: A theory for microtremor
478   H/V spectral ratio: Application for a layered medium. Geophysical Journal International, 186(1), 221–225,
479   2011.

480 Wittlinger, G., and Farra, V.: Observation of low shear wave velocity at the base of the polar ice sheets:
481   evidence for enhanced anisotropy. Geophysical Journal International, 190(1): 391–405, 2012.

482 Wittlinger, G., and Farra, V.: Evidence of unfrozen liquids and seismic anisotropy at the base of the polar ice
483   sheets. Polar Science 9.1: 66–79, 2015.

484 Yan, P., Li, Z. W., Li, F., Yang, Y. D., Hao, W. F., and Zhou, L.: Antarctic ice sheet thickness study based on
485   teleseismic receiver function. Chinese Journal of Geophysics, in press, 2017.

486

487

488   Table 1 Ice thickness results obtained from this study

489   (Thickness I, II are ice thickness values obtained from Eq. (1) and model B, respectively)

Station	Resonance freq. (Hz)	Thickness I (km)	Thickness II (km)	Bedmap2 (km)	Station	Resonance freq. (Hz)	Thickness I (km)	Thickness II (km)	Bedmap2 (km)
BENN	0.222±0.034	2.14±0.33	1.73	1.56	N124	0.185±0.019	2.56±0.26	2.57	2.42
BYRD	0.222±0.022	2.14±0.21	2.33	2.16	N132	0.146±0.018	3.26±0.40	3.07	3.24
E012	0.418±0.052	1.14±0.14	1.03	1.05	N140	0.162±0.022	2.93±0.42	2.69	2.79
E014	0.914±0.085	0.52±0.05	0.60	0.66	N148	0.137±0.017	3.46±0.44	3.20	2.90
E018	0.222±0.028	2.14±0.27	1.72	1.50	N156	0.194±0.016	2.45±0.20	2.48	2.55
E020	0.200±0.011	2.38±0.13	2.01	1.75	N165	0.150±0.021	3.16±0.44	2.95	2.81
E024	0.200±0.019	2.38±0.22	2.09	1.83	N173	0.185±0.017	2.56±0.24	2.54	2.38
E026	0.215±0.028	2.2±0.29	1.61	1.40	N182	0.191±0.014	2.49±0.19	2.54	2.42
E028	0.188±0.032	2.5±0.44	1.85	1.61	N190	0.144±0.017	3.31±0.41	3.15	3.01
E030	0.177±0.024	2.68±0.37	2.32	2.02	N198	0.148±0.017	3.21±0.38	3.30	3.32
GM01	0.155±0.018	3.07±0.36	3.12	3.10	N206	0.159±0.022	2.98±0.41	2.61	2.96
GM02	0.159±0.014	2.98±0.26	2.94	2.81	N215	0.155±0.017	3.07±0.33	3.12	3.48
GM03	0.159±0.018	2.98±0.33	2.88	2.52	P061	0.135±0.018	3.52±0.46	3.17	3.16
GM04	0.157±0.015	3.02±0.29	3.08	2.80	P071	0.194±0.018	2.45±0.23	2.18	2.30
GM05	0.146±0.020	3.26±0.45	3.17	3.47	P080	0.188±0.018	2.52±0.25	2.52	2.47
GM06	0.150±0.015	3.16±0.32	3.10	3.47	P090	0.212±0.022	2.24±0.23	2.09	2.34
GM07	0.148±0.012	3.21±0.26	3.08	3.03	P116	0.222±0.023	2.14±0.22	1.93	2.00
JNCT	0.349±0.031	1.36±0.12	1.26	1.19	P124	0.314±0.033	1.51±0.16	1.47	1.54
N020	0.222±0.021	2.14±0.21	1.95	1.71	ST01	0.157±0.015	3.02±0.28	2.95	3.02
N028	0.197±0.020	2.41±0.25	2.24	2.06	ST02	0.164±0.018	2.89±0.32	2.43	2.12
N036	0.152±0.020	3.12±0.41	2.53	2.21	ST03	0.236±0.019	2.01±0.16	2.86	2.49
N044	0.169±0.023	2.81±0.39	2.51	2.21	ST08	0.152±0.016	3.12±0.34	2.50	2.18
N052	0.152±0.022	3.12±0.45	2.75	2.39	ST09	0.157±0.020	3.02±0.4	2.66	2.32
N068	0.155±0.014	3.07±0.28	2.98	2.87	ST10	0.266±0.030	1.79±0.21	1.51	1.23
N076	0.172±0.014	2.76±0.23	2.59	2.46	ST12	0.185±0.020	2.56±0.28	2.15	1.89
N084	0.183±0.016	2.60±0.23	2.59	2.47	ST13	0.167±0.018	2.85±0.32	2.23	1.94
N092	0.175±0.016	2.72±0.25	2.48	2.63	ST14	0.339±0.038	1.40±0.16	1.44	1.54
N100	0.167±0.015	2.85±0.26	2.68	2.68	SWEI	0.162±0.017	2.93±0.31	2.93	2.84
N108	0.177±0.014	2.68±0.21	2.56	2.45	TIMW	0.175±0.020	2.72±0.32	2.65	2.57
N116	0.175±0.024	2.72±0.39	2.46	2.50	WAIS	0.127±0.015	3.73±0.43	3.71	3.37

490
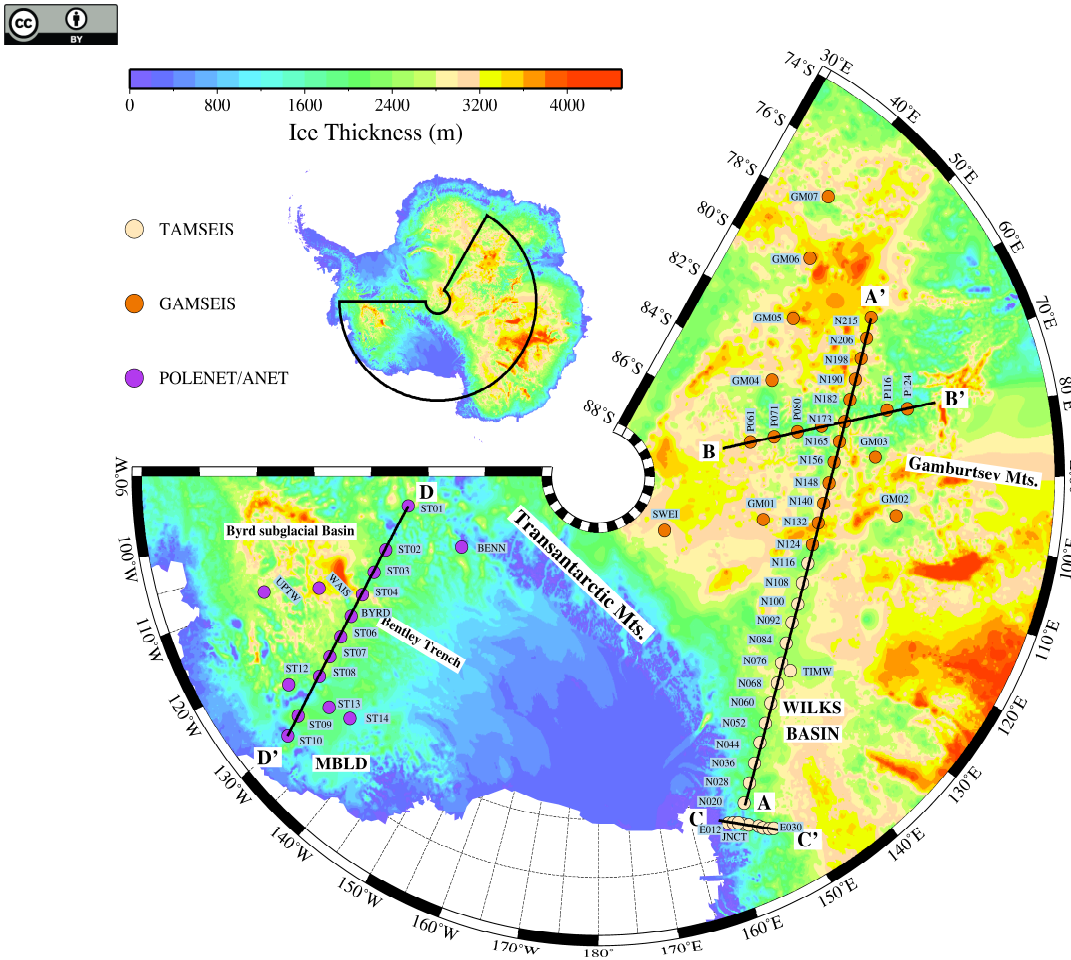
Figure 1. Locations of the three seismic arrays used in this study. Some stations are lined to four profiles marked with AA',
BB', CC' and DD'. TAMSEIS:TransAntarctic Mountains Seismic Experiment; GAMSEIS:Gamburtsev Antarctic
Mountains Seismic Experiment; POLENET/ANET:The Polar Earth Observing Network/Antarctic Network. Ice sheet
thickness data in this plot come from Bedmap2 database.

497

498
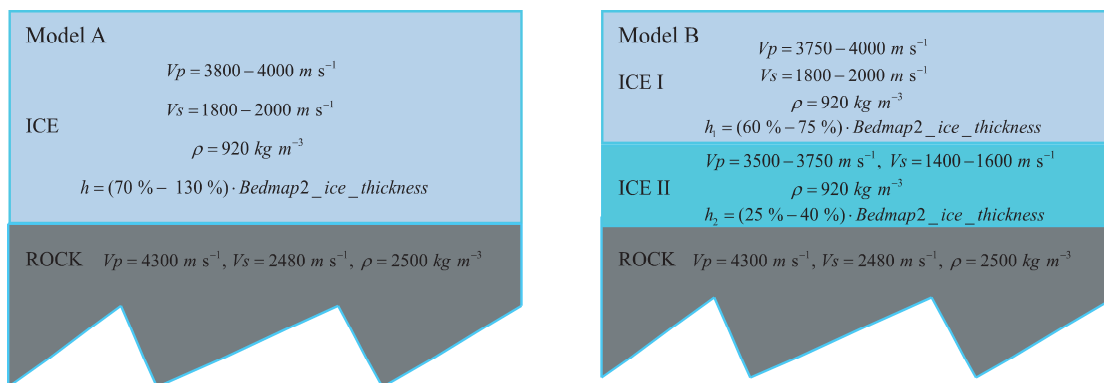
499 **Figure 2.** Sketches of the two ice layer models used for H/V spectrum inversion. Model A comprises a single ice layer,

500 while model B is a two-layer ice structure with low shear-wave velocity in the lower ice layer. The parameters used in the

501 two models are referred to Wittlinger (2012).

502

503

504
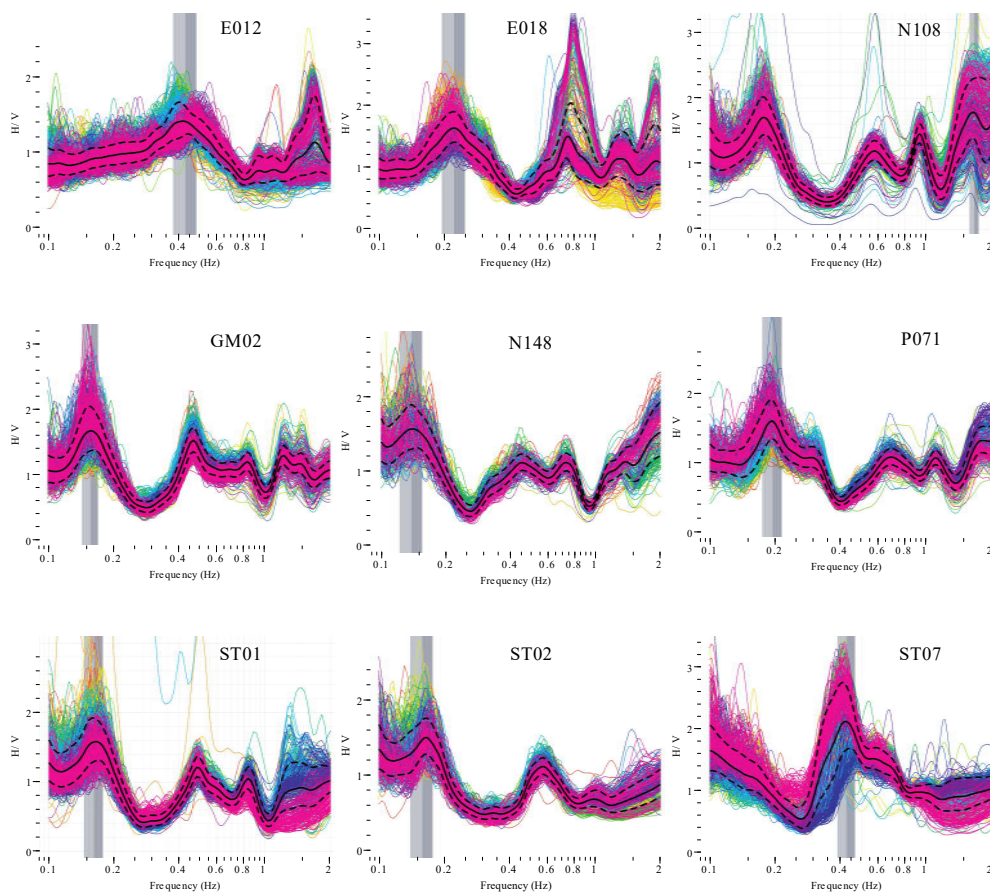
Figure 3. H/V spectra of nine stations shown as representative of all results in this study. The H/V spectra were calculated using five-day long ambient noise record. The spectra of the E012, E018, GM01, N148, P071, ST01 and ST02 stations represent 42 stations whose clear first peaks with the largest amplitudes are in agreement with the resonance frequency of the ice sheet layer. Station N108 is representative of 18 stations whose first peaks are related to the ice sheet resonance frequency but with slightly lower amplitude than peaks in higher frequencies. ST07 is the example that no peak frequency correlating to the ice thickness appears as expected in the observed H/V spectrum.

511

512

513
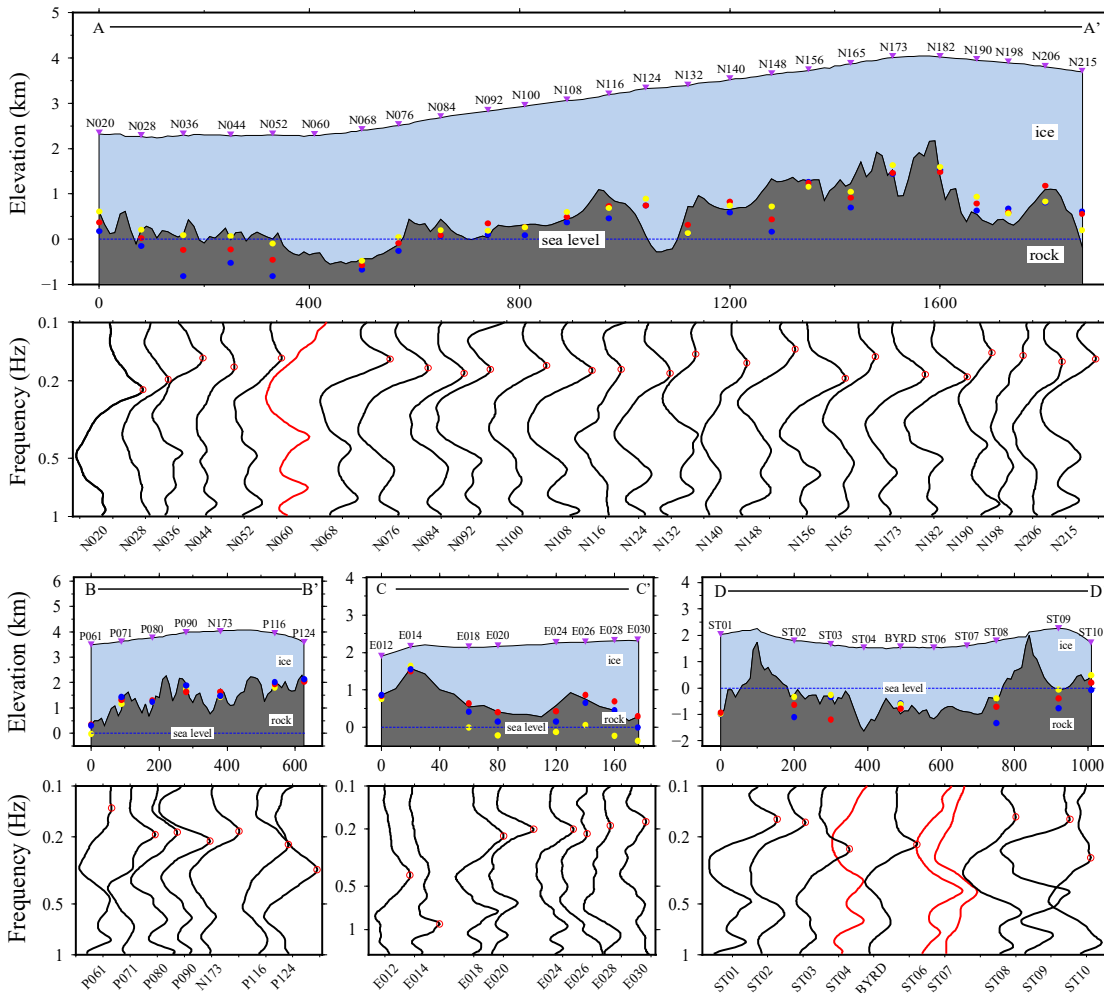
Figure 4. Cross section showing H/V spectra and the ice sheet thickness obtained from the H/V method at stations along the four profiles (Fig. 1). In the below H/V spectra cross section panels, the red circles denote the resonance frequencies correlating to the ice thickness for each station, and the spectra of the four stations without clear peaks are plotted with red lines. The upper panels show the variation of the bedrock and ice surface elevation along each profile obtained from Bedmap2 database. In these plots, the red dots indicate the reference Bedmap2 ice thickness, while the yellow and the blue dots represent the calculated ice thickness using Eq. (1) and the inversion ice thickness from model B, respectively.

520

521
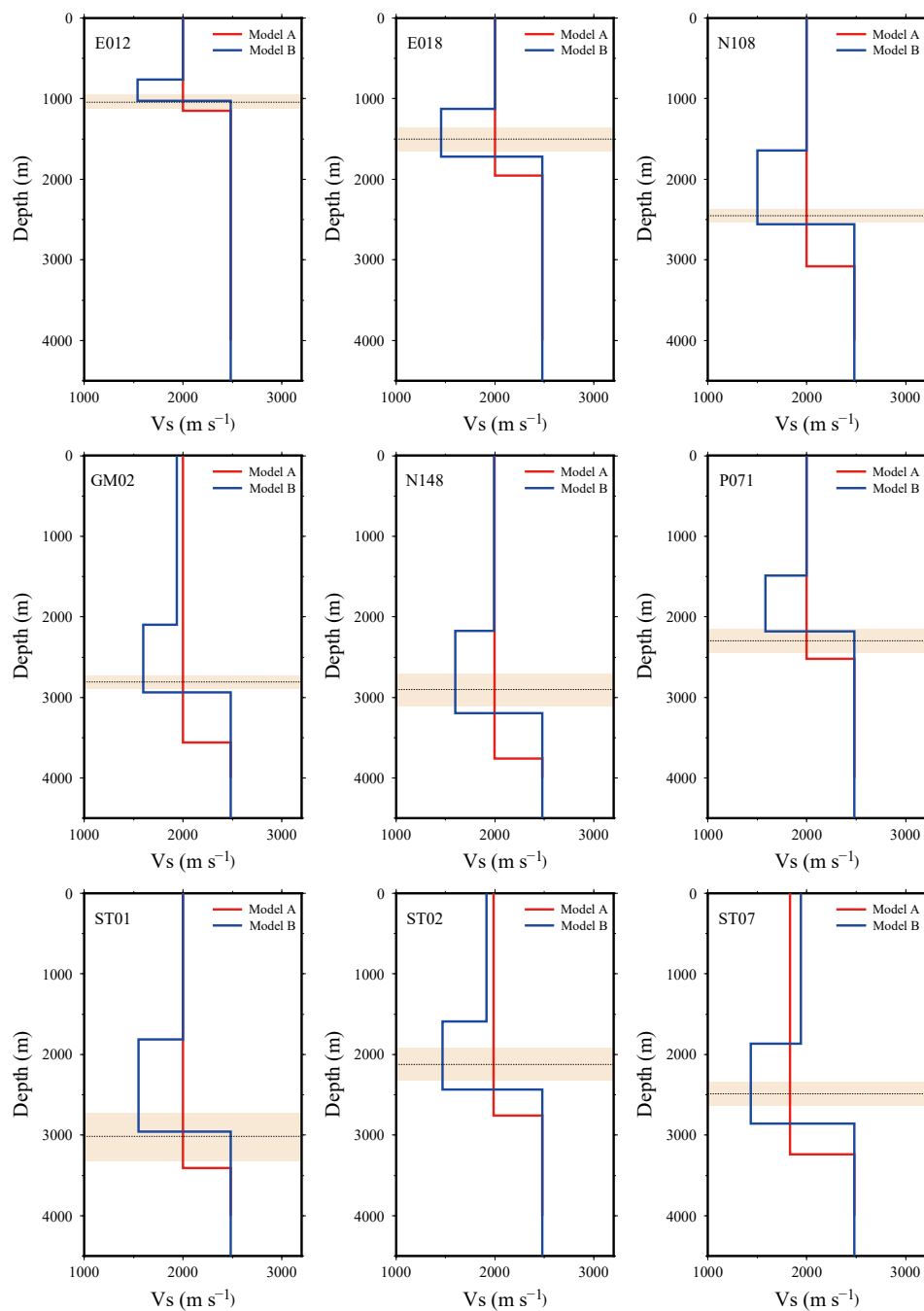
Figure 5. The optimum inversion shear-wave velocity models for the nine stations. The horizontal dashed line in each plot indicates the reference Bedmap2 ice thickness, and the shaded area shows the uncertainty of the Bedmap2 ice thickness. Apparently, the inversion ice thickness results derived from the two-layer structure (model B) are much closer to the Bedmap2 thickness than those determined using the single ice layer (model A).

527

528

529
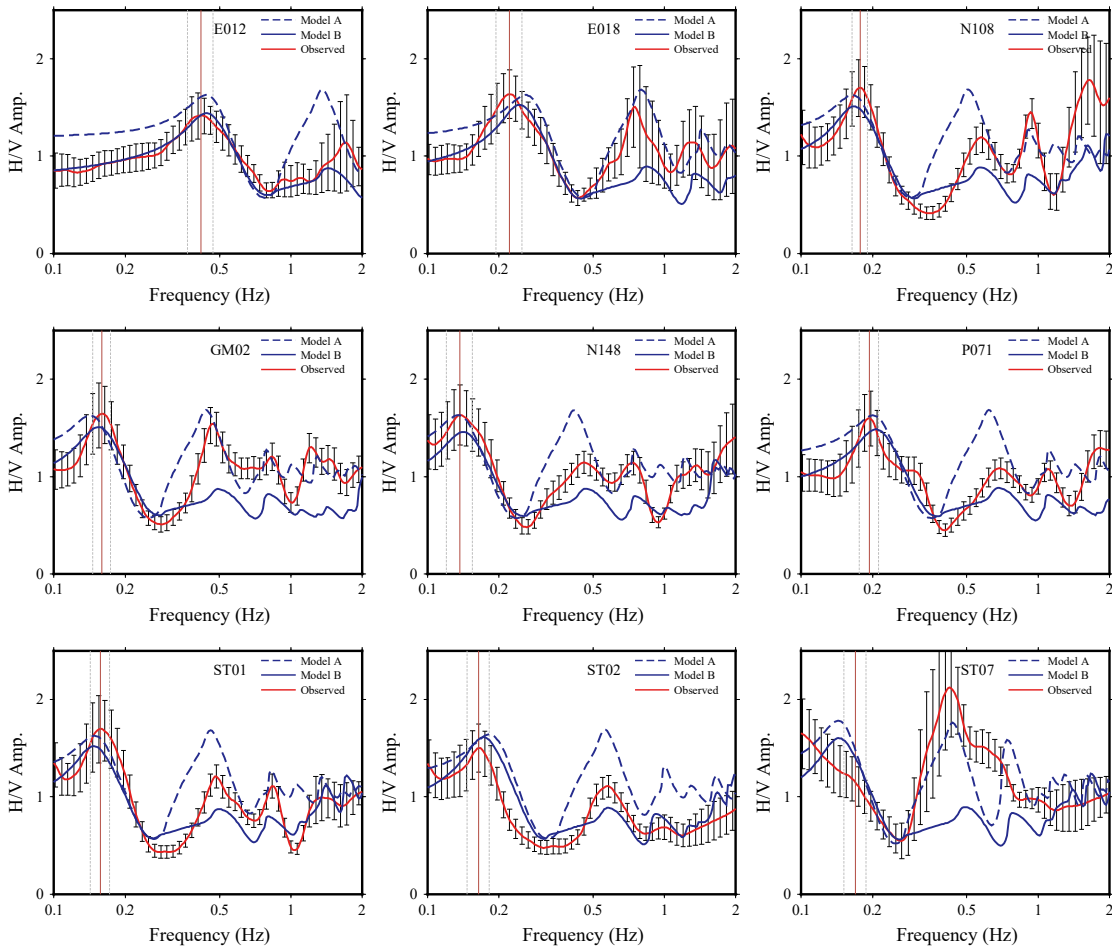
Figure 6. The synthetic H/V spectra and the observed H/V spectrum for the nine stations. The synthetic H/V spectra are
modelled using the optimum inversion shear-wave velocity profiles for model A and model B. The two synthetic H/V
spectra are both in good agreement with the observed H/V spectrum. Note that the amplitudes of the synthetic H/V spectra
are normalized by dividing 2 in the whole frequency band.

534

535

536
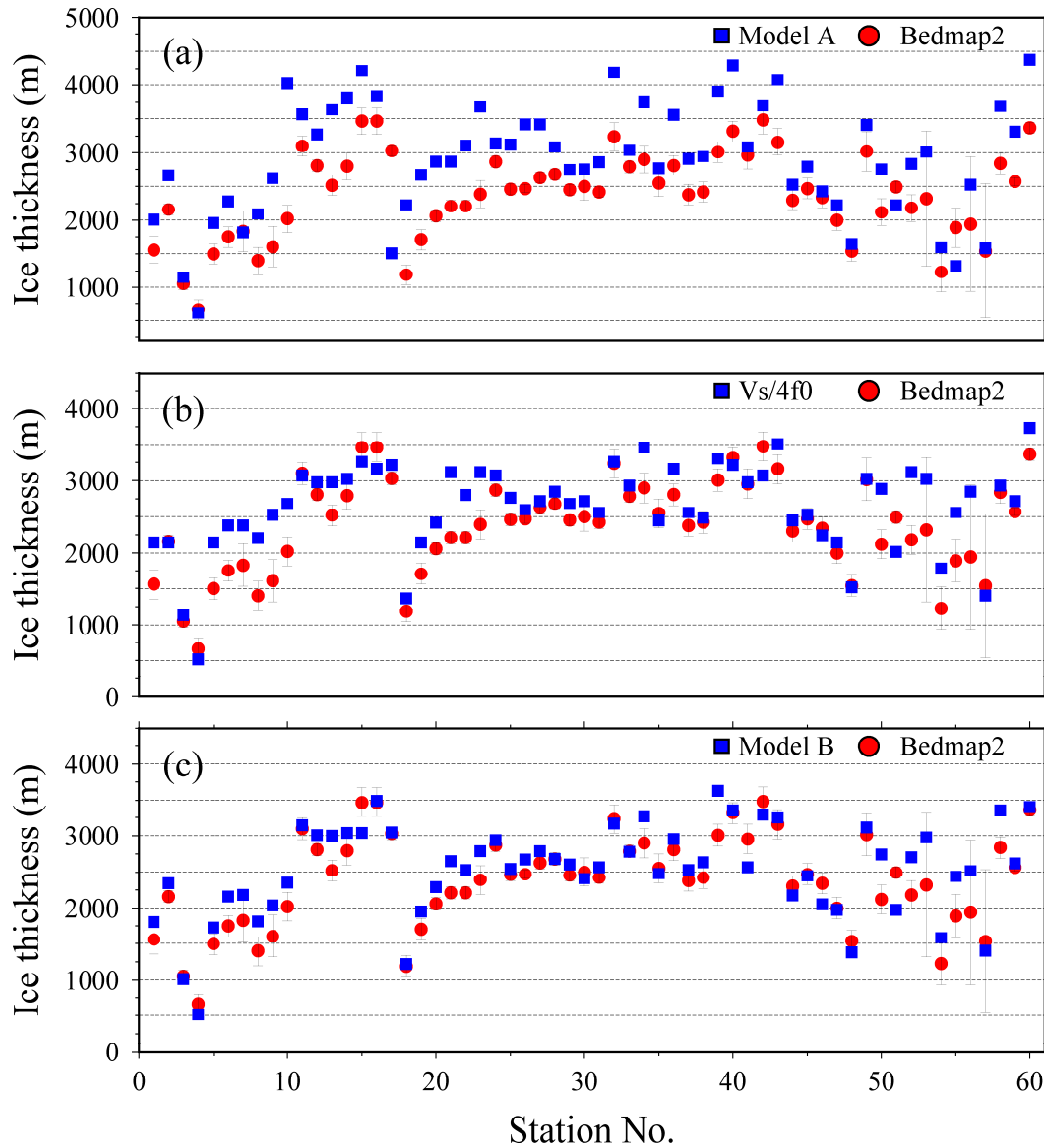
Figure 7. Ice thickness derived from the H/V method versus the reference Bedmap2 ice thickness. The blue squares in panel (a), (b), and (c) represent ice thickness estimations from model A, Eq. (1), and model B, respectively. The red circles in each panel denote the Bedmap2 ice thickness and each Bedmap2 value is marked with its corresponding error bar obtained from the uncertainty grids (Fretwell et al., 2013).

542

543
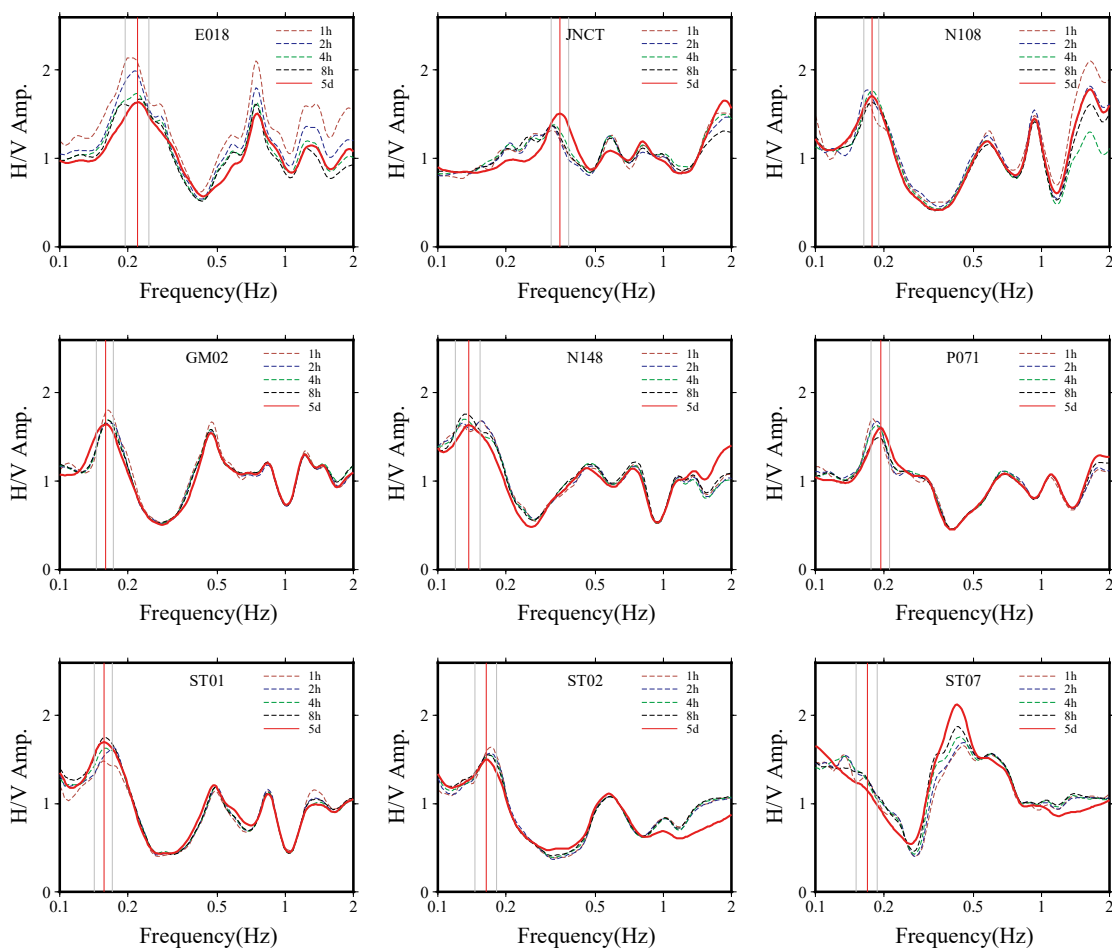
Figure 8. H/V spectra calculated using different lengths of ambient noise records. There is a good consistence between
H/V spectra determined with different tesing length of noise records (1 h, 2 h, 4 h and 8 h) and the spectrum with record
five-day long, both in locations of peak frequencies and the spectra shape. However, the peak frequency obtained from 1 h
record slightly deviates the peak frequency determined using 5 d record for the E012 station.

548

549

550
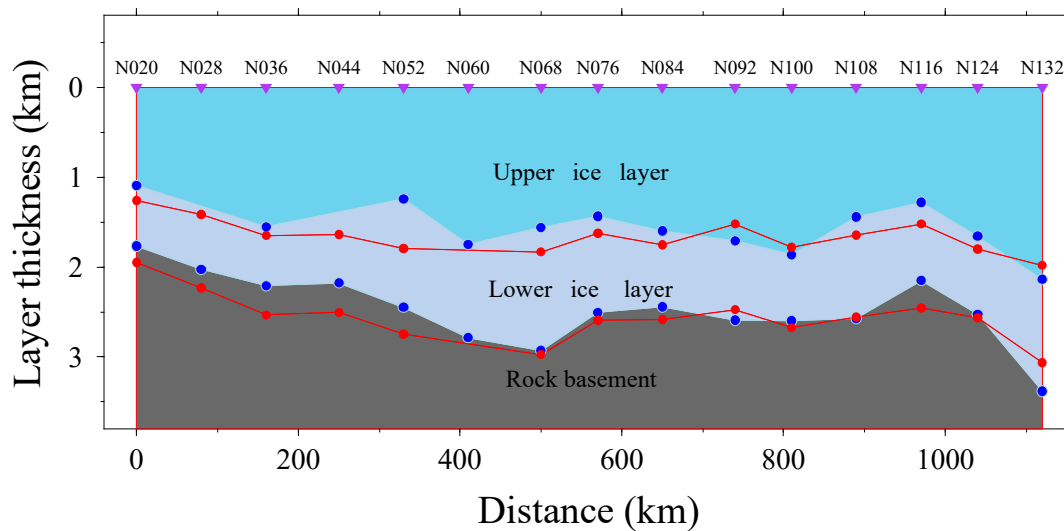
Figure 9. Comparisons of the two-layer ice thickness results obtained from our study and Wittlinger's. The red dots denote
the ice thickness derived from H/V spectrum inversion in our study, and the blue dots indicate the ice thickness determined
with the PRF method and a grid search stacking technique (Wittlinger and Farra, 2012, Table1).